

Theoretical study of an LAE-CIV absorption pair at $z = 5.7$

L. A. García^{1,2*}, E. Tescari^{2,3}, E. V. Ryan-Weber^{1,2} and J. S. B. Wyithe^{2,3}

¹Centre for Astrophysics and Supercomputing, Swinburne University of Technology, Hawthorn, VIC 3122, Australia

²ARC Centre of Excellence for All-Sky Astrophysics (CAASTRO)

³School of Physics, The University of Melbourne, Parkville, VIC 3010, Australia

Accepted XXX. Received YYY; in original form ZZZ

ABSTRACT

We present a theoretical model to predict the properties of an observed $z = 5.72$ Lyman α emitter galaxy – C IV absorption pair separated by 1384 comoving kpc/h. We use the separation of the pair and an outflow velocity/time travelling argument to demonstrate that the observed galaxy cannot be the source of metals for the C IV absorber. We find a plausible explanation for the metal enrichment in the context of our simulations: a dwarf galaxy with $M_{\star} = 1.87 \times 10^9 M_{\odot}$ located 119 comoving kpc/h away with a wind velocity of ~ 100 km/s launched at $z \sim 7$. Such a dwarf ($M_{UV} = -20.5$) is fainter than the detection limit of the observed example. In a general analysis of galaxy – C IV absorbers, we find galaxies with $-20.5 < M_{UV} < -18.8$ are responsible for the observed metal signatures. In addition, we find no correlation between the mass of the closest galaxy to the absorber and the distance between them, but a weak anti-correlation between the strength of the absorption and the separation of galaxy – absorber pairs.

Key words: Galaxies – intergalactic medium – methods: numerical – quasars: metal absorption lines – cosmology: theory.

1 INTRODUCTION

There is an intrinsic connection between the formation and evolution of galaxies in the Universe and the properties of the gas in the intergalactic medium (IGM), such as its metallicity and ionization state. These properties are successfully reproduced by simulations that employ feedback models, in forms of radiative and kinetic winds, able to chemically enrich the outer regions of galaxies (Shen et al. 2013). The detection of galaxies that shape observations of the IGM provides information on the interplay of the outflowing winds from the star-forming regions and the gas in the outskirts that is photoionized and polluted by these feedback mechanisms.

One of the best ways to explore the properties of the gas in the IGM is by the detection of C IV absorption systems. Among other high-ionization states, C IV traces low-density regions in the IGM at temperatures of $T \gtrsim 10^4$ K (Oppenheimer et al. 2009; Tescari et al. 2011; Cen & Chisari 2011; Finlator et al. 2015; Rahmati et al. 2016). In addition, C IV is a good indicator of ionized regions due to its large ionization potential energy and its detection in the spectra of background high redshift quasars (e.g. Danforth & Shull 2008; Ryan-Weber et al. 2009; Cooksey et al. 2010; Simcoe

et al. 2011; D’Odorico et al. 2013; Boksenberg & Sargent 2015; D’Odorico et al. 2016) from $z \sim 0$ to 6.

At low and intermediate redshift, extensive observational campaigns are carried out with the goal to find, identify and characterize galaxy – C IV absorbers pairs: at $z \sim 0.05$ by Burchett et al. (2016) and at $z \sim 2-3$ (Steidel et al. 2010; Turner et al. 2014). Observing these galaxy – C IV absorber systems when the Universe is approaching the tail of Reionization ($z \sim 6$), might give us a hint of the connection between the galaxies that drove the Reionization and the metal enrichment in the very early Universe. For example, Oppenheimer et al. (2009) explored the physical environment of the absorbers assuming different scenarios for the ionizing background and found that C IV absorbing gas is primarily intergalactic at $z \sim 6$. The absorbers are distributed at distances up to 200 physical kpc from the parent galaxy. In their HM2001 model, the C IV absorbers are only associated with galaxies of $M_{\star} \sim 10^9 M_{\odot}$. In addition, work from Oppenheimer et al. (2009); Finlator et al. (2016) showed that local sources can affect the strength of C IV absorption.

With the detection of a high redshift ($z = 5.72$) Lyman α emitting galaxy by Díaz et al. (2015, hereafter D15) located 212.8 physical kpc/h from a high column density ($\log N_{CIV}(\text{cm}^{-2}) = 14.52$) C IV absorber (D’Odorico et al. 2013), there is now observational evidence of a galaxy – absorber pair at this redshift. This detection opens the question: is

* E-mail: lgarcia@swin.edu.au

the C IV absorber due to an outflowing wind from the nearby star forming galaxy or does it instead arise due to an undetected dwarf galaxy closer to the line of sight?

A theoretical comparison with different feedback prescriptions at $z = 6$ by Keating et al. (2016) finds that their models are unable to reproduce the configuration observed by D15, and that their strong absorbers are linked to nearby galaxies (< 100 pkpc) with very high halo masses ($\log M_h/M_\odot \geq 10$). The low incidence rate of strong C IV absorption systems makes it doubly difficult to simulate the observed scenario. This letter is devoted to exploring the likelihood of reproducing a system as detected by D15 and to giving a plausible explanation for the enrichment. In addition, we make some theoretical predictions in order to guide the analysis of future observations.

The work follows the methodology and models described in García et al. (2017, MNRAS submitted; hereafter G17). The numerical simulations were run using a customized version of the smoothed particle hydrodynamics (SPH) code GADGET-3 (Springel 2005) with cosmological parameters from Planck Collaboration et al. (2016): $\Omega_{0m} = 0.307$, $\Omega_{0b} = 0.049$, $\Omega_\Lambda = 0.693$ and $H_0 = 67.74 \text{ km s}^{-1} \text{ Mpc}^{-1}$ (or $h = 0.6774$). The simulated run Ch 18 512 MDW has comoving box size and softening of 18 Mpc/h and 1.5 kpc/h, respectively, and includes 2×512^3 dark matter and gas particles. We assume a momentum-driven wind feedback model with a wind mass-loading factor $\eta = 2 \times \frac{600 \text{ km s}^{-1}}{v_w}$ and a velocity of $v_w = 2 \sqrt{\frac{GM_h}{R_{200}}} = 2 \times v_{\text{circ}}$.

The simulation has been post-processed with a field radiation due to the cosmic microwave background (CMB) and the Haardt & Madau (2012) ultraviolet/X-ray background from quasars and galaxies with saw-tooth attenuation (HM12), an effective prescription for HI self-shielding according to Rahmati et al. (2013), a photoionization modeling for C IV using Cloudy v8.1 (Ferland et al. 2013) for optically thin gas and Voigt profile fitting with the code Vpfit v.10.2 (Carswell & Webb 2014). As described in G17, our numerical simulations correctly reproduce observed global statistics of C IV absorbers, namely, the column density distribution function and the cosmological mass density $\Omega_{\text{C IV}}$. Throughout the paper, we use the prefix c for comoving and p for physical distances. Please note that in our simulation the closest snapshot to the $z = 5.72$ D15 system is at $z = 5.6$.

2 THE LAE – CIV ABSORPTION PAIR OF DÍAZ ET AL. 2015

In this section we investigate the likelihood of reproducing the galaxy – C IV absorber pair detected by D15 with theoretical models. Specifically, a C IV absorption system in the line of sight to the background quasar J1030+0524, with a column density of $\log N_{\text{C IV}} (\text{cm}^{-2}) = 14.52 \pm 0.08$ (D’Odorico et al. 2013) at a distance of $212.8^{+14}_{-0.4} h^{-1}$ pkpc (1384 ckpc/h in the adopted cosmology) from a Lyman α emitter galaxy (LAE) of $M_{\text{UV}} = -20.7$ at $z = 5.72$, with inferred parameters $\log (M_*/M_\odot) = 9.4$ (using the stellar mass function for $z = 6$ galaxies from Song et al. 2016) and $\log (M_h/M_\odot) = 10 - 11$ (derived from $z \sim 6.6$ LAE clustering from Ouchi et al. 2010). The possible scenarios

Table 1. Wind velocity (v_w) and travel time (t) to enrich a region at 1300 ckpc/h from our most massive galaxy (M_h).

Box size (cMpc/h)	M_h ($\times 10^{11} M_\odot$)	v_w (km/s)	t (Gyr)
18	4.9	446	0.73

that the authors propose to explain the metal enrichment of the region (in particular with Carbon) are either a very powerful galactic outflow that left the LAE at earlier times or an undetected dwarf galaxy closer to the absorber.

In the simulations, the chemical enrichment is driven by supernovae that produce and expel metals to the outer regions of galaxies. Wind velocities in the adopted feedback model depend on the halo mass of the galaxies. Therefore, only the most massive objects produce winds powerful enough to pollute regions at more than 1 cMpc/h, but these objects are quite rare at high redshift, especially in small simulations. We calculate the wind velocity and travel time of the most massive galaxy in the box in Table 1 to set an upper limit on the time required for an outflow to reach a region at a distance of 1300 ckpc/h (comparable to the D15 example). The results from Table 1 suggest that not even the most massive galaxy is able to produce winds with the velocity required to travel 1300 ckpc/h in a reasonable time. The time displayed in Table 1 is comparable with the age of the Universe at $z = 5.6$. Thus, for this option to be viable, galaxies would need to be formed at an age ($z \geq 30$) incompatible with the current paradigm of galaxy formation. Therefore, we rule out the possibility that an outflow produced by the LAE enriched a region at 1384 ckpc/h in the context of the feedback model implemented in our simulations. Nevertheless, alternative configurations could lead to a different result: more aggressive prescriptions for supernova-driven outflows or larger halo masses that produce higher wind velocities. The latter condition could be fulfilled in our simulations with a galaxy halo mass of $\sim 1.5 \times 10^{12} M_\odot$. However, galaxies have only been observed with stellar masses up to $10^{10} M_\odot$ at $z \sim 6$ (Song et al. 2016). Assuming a mass-to-light ratio of 10 (inferred from the simulations at this redshift), this scenario is still out of reach by at least an order of magnitude.

This test also reveals interesting details of the model: the chemical enrichment is driven by galaxies nearby the absorbers, since galactic outflows cannot travel a distance larger than about 1 cMpc in less than 0.5 Gyr and chemically enrich the IGM. At this redshift, active galactic nuclei are the only sources energetic enough to produce winds that travel that far.

Next, we explore the dwarf galaxy scenario, in which the presence of another galaxy closer to the absorber, and fainter than the detection limits for optical observations, is responsible for the enrichment. The upper limit for an undetected galaxy is: $M_{\text{UV}} = -20.5$, corresponding to $M_* = 10^{9.3} M_\odot$ (Song et al. 2016). Independent narrow band observations of Ly α emission set a limit on the star formation rate, $\text{SFR} = 5\text{--}10 M_\odot/\text{yr}$. The goal of this analysis is to find mock scenarios that resemble the conditions of the LAE detected in D15 and, if possible, confirm or rule out

the hypothesis of an undetected dwarf galaxy.

At $z = 5.6$, the simulated galaxies have halo masses in the range of $7.83 < \log M_h(M_\odot) < 10.83$. We classify them in the following categories: LAE candidates ($M_h \geq 1.48 \times 10^{10} M_\odot$) and dwarf galaxies ($1.48 \times 10^9 M_\odot < M_h < 1.48 \times 10^{10} M_\odot$) to provide a fair comparison with the observational parameters. Galaxies with halo mass below $1.48 \times 10^9 M_\odot$ are excluded from the statistics because of their low resolution. We stress that we do not follow the Ly α emission of any galaxy. The criterion to describe the galaxies is based only on their stellar and halo masses.

Stochastically, 1000 galaxies are selected from the friends-of-friends catalogue and from each one, a line of sight is projected with a random impact parameter d up to 1500 ckpc/h. The column density N_{CIV} and the position of the absorption in the box is recovered in each case. We focus on CIV absorption systems with $\log N_{\text{CIV}}(\text{cm}^{-2})$ in the range of 14-15. We then look for all the galaxies around the absorption (our absorption spectra have an uncertainty of 7 km/s, or ± 49 ckpc/h, along the line of sight). This set of galaxies is identified and sorted by mass and distance (the 3D distance can be decomposed in components parallel and perpendicular to the line of sight). The array in mass allows us to tag the galaxy as LAE or dwarf (or just exclude it according to the resolution criterion mentioned above), whereas the distance array defines the closest galaxies to the absorption. The cross-matching of the arrays leaves 4 systems with a configuration LAE – CIV absorption – dwarf galaxy, close to the observational arrangement.

In particular, one system drew our attention for its geometry being closest to the D15 observations. We show the configuration LAE – CIV absorption – dwarf galaxy in Figure 1. The CIV absorption feature has $\log N_{\text{CIV}}(\text{cm}^{-2}) = 14.3 \pm 1.1$, the LAE has $M_h = 1.54 \times 10^{10} M_\odot$ at a 3D distance of 1296 ckpc/h from the CIV system. The closest galaxy in the field, a dwarf galaxy of $M_* = 1.87 \times 10^9 M_\odot$, $M_h = 9.67 \times 10^9 M_\odot$, SFR = $0.07 M_\odot/\text{yr}$ is located at a 3D distance from the absorber of 119 ckpc/h. A dwarf galaxy with this stellar mass lies just below the 50% complete value for M_{UV} images of D15 at $M_* = 2 \times 10^9 M_\odot$. In this case, the velocity of an outflow produced by the dwarf galaxy is $v_w \sim 100$ km/s, leading to a travel time of ~ 260 Myr (*i.e.* the outflow was launched at $z \sim 7$). The spatial configuration displayed in Figure 1 favors an undetected dwarf galaxy in the observations of D15 and confirms that, in the context of our feedback model, the chemical enrichment is caused by nearby galaxies. In addition, these results emphasize that the metal absorption line systems offer the best technique for detecting galaxies beyond the limits of imaging at high redshifts.

As a final point, we mention that in the D15 observations, there is a small probability that an associated galaxy of any mass is obscured by the quasar. The highest resolution image of this quasar is an HST/ACS z-band image taken by Stiavelli et al. (2005). Conservatively, we estimate that the quasar light would prevent the detection of galaxies within a radius of 1 arcsec. Thus, 11% of the circular area within 18 pkpc/h (119 ckpc) from the quasar line of sight is obscured. At this redshift, a separation of 18 pkpc/h corresponds to 3.07 arcsec. In order to understand the incidence rate of galaxies around the CIV absorption in the particu-

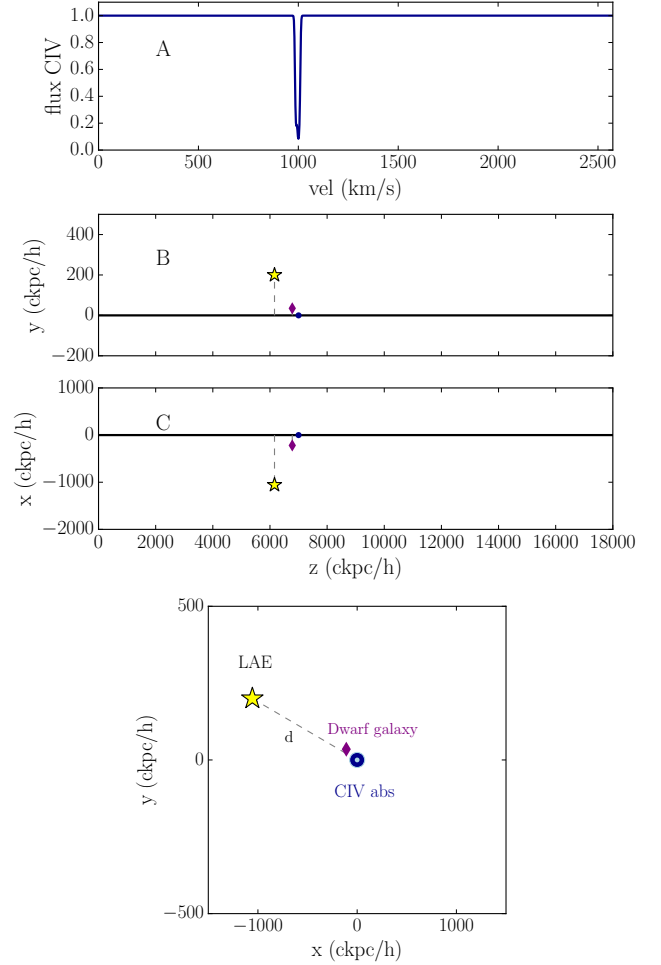


Figure 1. Theoretical example of the observed LAE – CIV absorption pair. In this window, we test one of the hypotheses proposed in D15: the existence of an undetected dwarf galaxy in the field of the LAE. We identify all the CIV absorptions at $z = 5.6$ with $\log N_{\text{CIV}}(\text{cm}^{-2})$ in the range of 14–15 and the closest galaxies in the surroundings of each absorption. The upper panel (A) shows a feature with $\log N_{\text{CIV}}(\text{cm}^{-2}) = 14.3 \pm 1.1$ on a line of sight traced along the z direction. Panel B shows the position of the strong CIV absorption (blue point), an LAE (yellow star) with $M_h = 1.54 \times 10^{10} M_\odot$ and a 3D distance of 1296 ckpc/h from the absorption, and the closest galaxy in the field (purple diamond), a dwarf galaxy of $M_* = 1.87 \times 10^9 M_\odot$ at a 3D distance from the absorber of 119 ckpc/h, that could not have been detected in the observations. Panel C shows the same configuration in a different edge-on projection (xz). The bottom panel displays the physical disposition of the system face-on: the line of sight from the quasar (in the background) contains the absorption and it is orthogonal to the plane of the image.

lar scenario discussed above, we plot the distribution of 3D distances from the absorption to each galaxy in a range of 1500 ckpc/h in Figure 2. There are many more dwarf galaxies closer to the CIV absorber than the LAE. Furthermore, the probability of finding a randomly placed dwarf galaxy at 119 ckpc/h from a metal absorber is 5.1%, knowing that the number density of dwarf galaxies in the sample is 0.46 objects per cMpc^3 and the volume where these pairs are likely to occur is about 0.02 cMpc^3 .

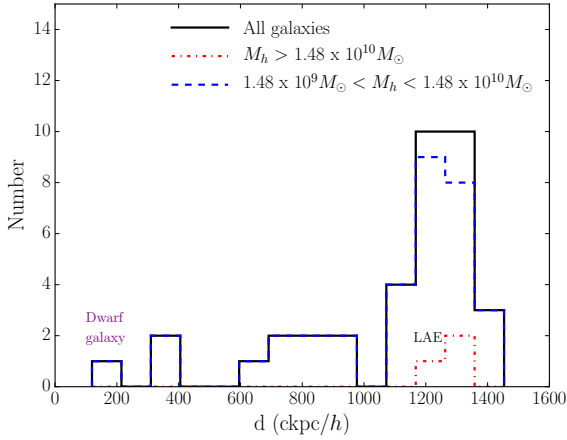


Figure 2. Distribution of galaxies around the CIV strong absorption shown in Figure 1 up to a 3D distance of 1500 ckpc/h. The black histogram accounts for all galaxies, whereas the red dashed–dotted line shows the systems with masses $M_h \geq 1.48 \times 10^{10} M_\odot$ (LAE) and the blue dashed line the contribution from dwarf galaxies $1.48 \times 10^9 < M_h/M_\odot < 1.48 \times 10^{10}$ in the box. The galaxies below the mass resolution limit of $1.48 \times 10^9 M_\odot$ are not shown.

3 GALAXY – ABSORBER CONNECTION

We have shown a theoretical realization of the observed LAE – CIV absorption pair at $z = 5.6$. Now, we want to explore the physical connection of these systems (if any), using the properties of the galaxies and the column densities of the absorbers in the simulated box. For the purpose of the analysis of this section, which is made with galaxies in the simulations above the mass resolution limit, we define high ($M_h \geq 1.48 \times 10^{10} M_\odot$), intermediate ($6.64 \times 10^9 < M_h/M_\odot < 1.48 \times 10^{10}$) and low mass ($1.48 \times 10^9 < M_h/M_\odot < 6.64 \times 10^9$) galaxies.

The connection of the galaxy – CIV systems can be studied using galaxy – absorber pairs with $\log N_{CIV} (\text{cm}^{-2}) > 13$ and taking into account the nearest galaxy to the absorption. We implicitly assumed that this nearest galaxy is the main source of metal enrichment for the absorber.

We construct the overall distribution of the distance from each absorption to its closest galaxy in the simulated box. From the initial sample of 1000 lines of sight, 182 CIV absorbers have a galaxy companion above the mass resolution. In Figure 3, we display this distribution with respect to the mass of the galaxy.

There are not high mass galaxies in the random selection from the friends-of-friends catalogue because just 2% of the objects are in the range of mass $M_h \geq 1.48 \times 10^{10} M_\odot$, which makes it extremely hard to encounter a random line of sight through these galaxies. On the other hand, almost 90% of the galaxies in the box are intermediate and low mass ($1.48 \times 10^9 < M_h/M_\odot < 1.48 \times 10^{10}$). Therefore, it is not surprising that the closest galaxy to each $N > 10^{13} \text{ cm}^{-2}$ CIV absorber has a mass in this range.

Additionally, intermediate and low mass galaxies are typically found at a mean distance of 520 ckpc/h (78.8 pkpc/h) and 700 ckpc/h (106.1 pkpc/h), respectively. This result is

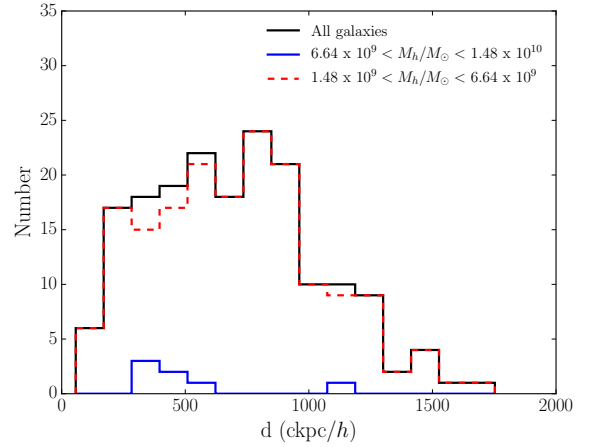


Figure 3. Mass distribution of the 3D distance from the CIV absorptions to the closest galaxy. The black histogram accounts for all the galaxies. There are not high mass galaxies ($M_h \geq 1.48 \times 10^{10} M_\odot$), meaning that, in all cases, the closest galaxies from the absorptions lay in the category of dwarfs. Intermediate mass galaxies are presented in blue solid line (7) and low mass galaxies with dashed red (175). The galaxies below the mass resolution limit $1.48 \times 10^9 M_\odot$ are not presented. In cases where $d \geq 1500$ ckpc/h, the enrichment is most likely due to an unresolved galaxy.

only partially in agreement with findings of [Oppenheimer et al. \(2009\)](#), for high stellar-mass galaxies in their HM2001 model: strong CIV absorptions at $z = 6.0$ are associated with galaxies with $M_* \sim 10^9 M_\odot$ and the typical galaxy – absorption separation is less than 100 pkpc. It is important to clarify that, in addition to the intrinsic difference between HM2001 and HM12 backgrounds, their highest mass galaxies are close to our mass resolution (lower) limit. Nonetheless, we confirm that CIV is mostly found in the IGM (G17; [Oppenheimer et al. 2009](#)). Finally, Figure 3 reveals that the CIV strong absorptions at high redshift are driven by dwarf galaxies with M_* spanning the range $10^{8.46-9.42} M_\odot$ and $\text{SFR}=0.01-2.5 M_\odot/\text{yr}$. These parameters allow us to infer an absolute magnitude M_{UV} in the range of (-20.5,-18.8) (using the $M_* - M_{UV}$ relation at $z \sim 6$ from [Song et al. 2016](#)) that should be achieved with future surveys. The detection and study of these faint galaxies is fundamental, since they are believed to provide the largest contribution of photons to complete the Reionization of Hydrogen ([Robertson et al. 2015](#); [Liu et al. 2016](#)).

Figure 4 shows the distribution of 3D distance from the CIV absorptions to the closest galaxy as a function of column density of the absorption. The 182 absorbers span the range of $13 \leq \log N (\text{cm}^{-2}) \leq 16$. From this sample, there are 73 absorbers with $13 \leq \log N (\text{cm}^{-2}) < 14$, 31 in the range of $14 \leq \log N (\text{cm}^{-2}) < 15$ and 78 with $\log N (\text{cm}^{-2}) \geq 15$. The mean distance in the three cases is respectively: 710.6, 705.5 and 680.6 ckpc/h. This result indicates that there is a weak negative correlation between the column density of the CIV absorptions and the separation of absorber – galaxy pairs.

Finally, it is worth noting that strong CIV absorptions in our simulations are produced not only by very close struc-

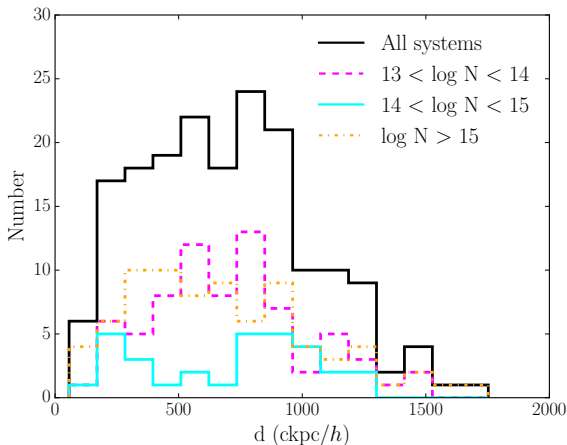


Figure 4. Distribution of the 3D distance from the CIV absorptions to the closest galaxy with respect to the column density of the absorption. The black histogram accounts for all the column densities in the range of $13 \leq \log N \text{ (cm}^{-2}\text{)} \leq 16$. The magenta dashed line shows systems with $13 \leq \log N \text{ (cm}^{-2}\text{)} < 14$, the cyan solid line the systems with $14 \leq \log N \text{ (cm}^{-2}\text{)} < 15$ and in orange dashed-dotted line systems with column densities $\log N \text{ (cm}^{-2}\text{)} \geq 15$.

tures with large masses ($M_h \sim 10^{10-11} M_\odot$, which we rarely find within this box size), but also for small galaxies.

4 CONCLUSIONS

We have explored the likelihood of reproducing the observed LAE – CIV absorption pair detected by D15 and studied the physical processes that produced the metal enrichment in the IGM at $z \sim 5.6$. In the context of our feedback model, we rule out the scenario of an outflow produced by the observed LAE at a distance of 1384 ckpc/h at early times.

Instead, our simulations support a scenario in which a dwarf galaxy, undetected in the field, very close to the absorber (119 ckpc/h), with $M_* = 1.87 \times 10^9 M_\odot$, $M_h = 9.67 \times 10^9 M_\odot$ and $\text{SFR} = 0.07 M_\odot/\text{yr}$, is responsible for the CIV absorption.

Additionally, we find that the main drivers of the chemical enrichment of the IGM and CIV strong absorptions at $z = 5.6$ are dwarf galaxies, which are mostly observed at a mean distance of 700 ckpc/h (106.1 pkpc/h). These galaxies have stellar masses M_* in the range $10^{8.46-9.42} M_\odot$ and $\text{SFR} = 0.01-2.5 M_\odot/\text{yr}$. From these parameters, we infer an absolute magnitude M_{UV} in the range of (-20.5,-18.8), derived by combining results of Song et al. (2016) with the Kennicutt relation. Future observations and investigations of these faint galaxies are fundamental, since they are believed to be the largest contributors of photons to the Reionization of Hydrogen.

When exploring the galaxy – absorber connection at high redshift, we find no correlation between the mass of the closest galaxy to the absorber and the distance between them. On the other hand, we encounter a weak negative correlation between the column density and the separation

of the galaxy – absorber pairs. The largest column densities are preferentially seen when separations are smallest.

Parts of this research were conducted by the Australian Research Council Centre of Excellence for All-sky Astrophysics (CAASTRO), through project number CE110001020. This work was supported by the Flagship Allocation Scheme of the NCI National Facility at the ANU. The authors acknowledge CAASTRO for funding and allocating time for the project **Diagnosing Hydrogen Reionization with metal absorption line ratios** (fy6) during 2015 and 2016. We also thank the anonymous referee for their insightful comments. ERW acknowledges ARC DP 1095600.

REFERENCES

- Boksenberg A., Sargent W. L. W., 2015, *ApJS*, **218**, 7
- Burchett J., Tripp T. M., Bordoloi R., Willmer C., 2016, in American Astronomical Society Meeting Abstracts. p. 109.08
- Carswell R. F., Webb J. K., 2014, VPFIT: Voigt profile fitting program, Astrophysics Source Code Library (ascl:1408.015)
- Cen R., Chisari N. E., 2011, *ApJ*, **731**, 11
- Cooksey K. L., Thom C., Prochaska J. X., Chen H.-W., 2010, *ApJ*, **708**, 868
- D’Odorico V., et al., 2013, *MNRAS*, **435**, 1198
- D’Odorico V., et al., 2016, *MNRAS*, **463**, 2690
- Danforth C. W., Shull J. M., 2008, *ApJ*, **679**, 194
- Díaz C. G., Ryan-Weber E. V., Cooke J., Koyama Y., Ouchi M., 2015, *MNRAS*, **448**, 1240
- Ferland G. J., et al., 2013, *Rev. Mex. Astron. Astrofis.*, **49**, 137
- Finlator K., Thompson R., Huang S., Davé R., Zackrisson E., Oppenheimer B. D., 2015, *MNRAS*, **447**, 2526
- Finlator K., Oppenheimer B. D., Davé R., Zackrisson E., Thompson R., Huang S., 2016, *MNRAS*, **459**, 2299
- García L. A., Tesfari E., Ryan-Weber E. V., Wyithe J. S. B., 2017, *MNRAS* submitted
- Haardt F., Madau P., 2012, *ApJ*, **746**, 125
- Keating L. C., Puchwein E., Haehnelt M. G., Bird S., Bolton J. S., 2016, *MNRAS*, **461**, 606
- Liu C., Mutch S. J., Angel P. W., Duffy A. R., Geil P. M., Poole G. B., Mesinger A., Wyithe J. S. B., 2016, *MNRAS*, **462**, 235
- Oppenheimer B. D., Davé R., Finlator K., 2009, *MNRAS*, **396**, 729
- Ouchi M., et al., 2010, *ApJ*, **723**, 869
- Planck Collaboration et al., 2016, *A&A*, **594**, A13
- Rahmati A., Pawlik A. H., Raičević M., Schaye J., 2013, *MNRAS*, **430**, 2427
- Rahmati A., Schaye J., Crain R. A., Oppenheimer B. D., Schaller M., Theuns T., 2016, *MNRAS*,
- Robertson B. E., Ellis R. S., Furlanetto S. R., Dunlop J. S., 2015, *ApJ*, **802**, L19
- Ryan-Weber E. V., Pettini M., Madau P., Zych B. J., 2009, *MNRAS*, **395**, 1476
- Shen S., Madau P., Guedes J., Mayer L., Prochaska J. X., Wadsley J., 2013, *ApJ*, **765**, 89
- Simcoe R. A., et al., 2011, *ApJ*, **743**, 21
- Song M., et al., 2016, *ApJ*, **825**, 5
- Springel V., 2005, *MNRAS*, **364**, 1105
- Steidel C. C., Erb D. K., Shapley A. E., Pettini M., Reddy N., Bogosavljević M., Rudie G. C., Rakic O., 2010, *ApJ*, **717**, 289
- Stiavelli M., et al., 2005, *ApJ*, **622**, L1
- Tesfari E., Viel M., D’Odorico V., Cristiani S., Calura F., Borgani S., Tornatore L., 2011, *MNRAS*, **411**, 826
- Turner M. L., Schaye J., Steidel C. C., Rudie G. C., Strom A. L., 2014, *MNRAS*, **445**, 794

This paper has been typeset from a \TeX/L\AA\TeX file prepared by the author.